

## PREY TYPE CONSTRAINS GROWTH AND PHOTOSYNTHETIC CAPACITY OF THE KLEPTOPLASTIDIC CILIATE *MESODINIUM CHAMAELEON* (CILIOPHORA)<sup>1</sup>

Holly V. Moeller <sup>2</sup>, Veronica Hsu, Michelle Lepori-Bui, Lisa Y. Mesrop, Cara Chinn

Department of Ecology, Evolution, and Marine Biology, University of California - Santa Barbara, Santa Barbara  
 California 93106, USA

and Matthew D. Johnson

Biology Department, Woods Hole Oceanographic Institution, Woods Hole, Massachusetts 02543, USA

**Kleptoplastidic, or chloroplast-stealing, lineages offer insight into the process of acquiring photosynthesis. By quantifying the ability of these organisms to retain and use photosynthetic machinery from their prey, we can understand how intermediaries on the endosymbiosis pathway might have evolved regulatory and maintenance mechanisms. Here, we focus on a mixotrophic kleptoplastidic ciliate, *Mesodinium chamaeleon*, noteworthy for its ability to retain functional chloroplasts from at least half a dozen cryptophyte algal genera. We contrasted the performance of kleptoplastids from blue-green and red cryptophyte prey as a function of light level and feeding history. Our experiments showed that starved *M. chamaeleon* cells are able to maintain photosynthetic function for at least 2 weeks and that *M. chamaeleon* containing red plastids lost chlorophyll and electron transport capacity faster than those containing blue-green plastids. However, likely due to increased pigment content and photosynthetic rates in red plastids, *M. chamaeleon* had higher growth rates and more prolonged growth when feeding on red cryptophytes. For example, *M. chamaeleon* grew rapidly and extensively when fed the blue-green cryptophyte *Chroomonas mesostigmatica*, but this growth appeared to hinge on high levels of feeding supporting photosynthetic activity. In contrast, even starved *M. chamaeleon* containing red plastids from *Rhodomonas salina* could achieve high photosynthetic rates and extensive growth. Our findings show that plastid origin impacts the maintenance and magnitude of photosynthetic activity, though whether this is due to variation in ciliate control or gradual loss of plastid function in ingested prey cells remains unknown.**

**Key index words:** acquired phototrophy; cryptophyte algae; kleptoplasty; Mesodiniidae; mixotrophy

For eukaryotic organisms, the chloroplast, which contains key light-harvesting and carbon-fixing machinery, is the key organelle necessary for photosynthesis. Across the tree of life, many lineages bear permanent chloroplasts, including most terrestrial plants, macroalgae, and eukaryotic phytoplankton. Yet other lineages gain transient access to this photosynthetic machinery by retaining functional chloroplasts from the food that they eat (Stoecker et al. 2009, Johnson 2011a). Termed “kleptoplastidic” (or chloroplast-stealing), these lineages vary in the extent to which they rely on this acquired metabolism. Some taxa receive limited amounts of photosynthate from plastids that rapidly degrade within the new host’s cytoplasm, while others obtain the majority of their carbon from photosynthesis (Johnson 2011b).

The degree to which kleptoplastidic lineages receive photosynthetic benefits from their plastids is likely tied to both environmental conditions and regulatory mechanisms. For example, under high light conditions, photodamage can decrease the lifetime of kleptoplastids (Vieira et al. 2009, García-Portela et al. 2018) and limit their carbon contribution. But for lineages that can remodel or repair photosynthetic machinery, kleptoplastid function can be maintained over much longer periods of time (Johnson et al. 2006, Kim et al. 2015). Kleptoplastidic lineages capable of prolonged plastid retention may show true phototroph-like characteristics, such as the ability to photoacclimate (Moeller et al. 2011, Hansen et al. 2016) and/or synthesize new photosynthetic pigments (Johnson and Stoecker 2005, Kim et al. 2012). Lineages with prolonged retention of functional plastids also tend to exhibit a higher degree of prey specialization, consistent with more refined mechanisms of integrating prey plastids into metabolism (Flynn et al. 2019). However, comparing these traits across lineages to link traits to kleptoplastid function is challenging because kleptoplastidic taxa are phylogenetically diverse.

The *Mesodinium* genus of marine ciliates may allow for such comparative approaches because the genus contains at least six named species, which can be broadly grouped into three categories based on

<sup>1</sup>Received 21 August 2020. Revised 18 December 2020. Accepted 21 December 2020.

<sup>2</sup>Author for correspondence: e-mail: holly.moeller@lifesci.ucsb.edu  
 Editorial Responsibility: J. Raven (Associate Editor)

their extent of kleptoplasty (Garcia-Cuetos et al. 2012, Moestrup et al. 2012, Johnson et al. 2016, Moeller and Johnson 2018). *Mesodinium pulex* and *M. pupula* are heterotrophic; These predominantly benthic taxa feed on dinoflagellates as well as cryptophytes (Jakobsen et al. 2006, Tarangkoon and Hansen 2011) and do not retain prey plastids. In contrast, the *M. major/rubrum* species complex contains eight variants which retain plastids from a restricted set of phycoerythrin-bearing cryptophyte algae (Johnson et al. 2016). These kleptoplastids contribute > 95% of the ciliate's carbon (Johnson et al. 2006, Smith and Hansen 2007) and are maintained through active transcription of genes from a cryptophyte prey nucleus retained alongside the stolen chloroplasts (Johnson et al. 2007). Third, the phylogenetically intermediate lineages *M. chamaeleon* and *M. coatsi* are more mixotrophic in habit: These ciliates retain plastids from at least a half a dozen species of cryptophyte algae including both blue-green and red cryptophytes (Nam et al. 2014, Moeller and Johnson 2018, Kim et al. 2019), but appear to rely equally on heterotrophy and phototrophy for growth (Garcia-Cuetos et al. 2012, Moeller and Johnson 2018).

While *Mesodinium rubrum* has been relatively well-studied as a model kleptoplastidic lineage (reviewed in Hansen et al. 2013), less is known about the photosynthetic capabilities of *M. chamaeleon* or *M. coatsi*. We do know that kleptoplastid residence times appear to be shorter and that prey niche breadth appears to be wider than in *M. rubrum* (Moestrup et al. 2012, Moeller and Johnson 2018, Kim et al. 2019). Yet we understand less about how the mixotrophic growth of these ciliates differs as a function of light availability or prey type. Further, we have limited data on photophysiology, including comparisons of plastid performance and maintenance in the ciliate relative to the native (cryptophyte) host.

Here, we address this knowledge gap by studying the growth and photophysiology of *Mesodinium chamaeleon* as a function of two key limiting resources: prey and light. Because *M. chamaeleon* cells are typically found bearing blue-green plastids in nature (Moestrup et al. 2012, Moeller and Johnson 2018, Kim and Park 2019), our overarching hypothesis was that *M. chamaeleon* would have the highest performance (maintain photosynthetic capacity over longer periods of time, have the fastest growth rate, and achieve the greatest increase in abundance) when retaining plastids from blue-green cryptophyte algae. Therefore, we offered *M. chamaeleon* prey from four different genera of known cryptophyte prey (Kim and Park 2019): two (*Chroomonas major* and *Hemiselmis pacifica*) contain green (cryptophyte phycocyanin-bearing) plastids; and two (*Storeatula major* and *Rhodomonas salina*) contain red (cryptophyte phycoerythrin-bearing) plastids (Cunningham et al. 2019, Greenwold et al. 2019). We verified the retention of plastids from each of the four prey

types and contrasted photosynthetic performance of plastids in *M. chamaeleon* and their original cryptophyte host. Finally, we compared the growth of *M. chamaeleon* across prey types and light levels, and used measurements of photosynthesis and grazing to assess the contributions of phototrophy and heterotrophy to growth. Our results confirm *M. chamaeleon*'s relatively general ability to retain cryptophyte plastids, but indicate that variable plastid maintenance may underlie differential reliance on feeding across prey types.

## MATERIALS AND METHODS

*Cultures and maintenance conditions.* The *Mesodinium chamaeleon* strain used in this study (strain NRMC-1802) was isolated by Matthew D. Johnson from the Narrow River, Narragansett Bay, Rhode Island, USA, in July 2018. *Mesodinium chamaeleon* stock cultures are maintained in 0.2  $\mu\text{m}$  filtered coastal seawater from Santa Barbara, California, USA (salinity of 35, pH = 7.8) at 18°C with a 12:12 h light:dark diel cycle in incubators (Percival Scientific Model I-36LLVL, Perry, IA, USA) with illumination from fluorescent bulbs (Philips Alto, 4100 Kelvin color temperature, Philips Lighting Company, Somerset, NJ, USA). All experiments were conducted at this temperature and light cycle. Prey stock cultures were maintained under the same light and temperature regime in f/2-Si amended seawater (Guillard 1975). Three prey cultures, *Chroomonas mesostigmatica* (CCMP 1168), *Hemiselmis pacifica* (CCMP 706), and *Rhodomonas salina* (CCMP 757), were obtained from the National Center for Marine Algae and Microbiota (NCMA, Bigelow Laboratory, East Boothbay, ME). The fourth, *Storeatula major* (strain SM or g) was isolated by Alan Lewitus from the Choptank River, Cambridge, MD, USA.

Prior to beginning any experiments *Mesodinium chamaeleon* were acclimated to each prey type for a period of at least 2 months to avoid the effects of remaining plastids from another prey type (Moeller and Johnson 2018). To avoid the confounding effects of short-term photoacclimatory responses, both prey and *M. chamaeleon* were also conditioned to experimental light levels of 10, 50, or 100  $\mu\text{mol quanta} \cdot \text{m}^{-2} \cdot \text{s}^{-1}$  for at least 3 weeks.

*Experimental design.* We conducted a fully-factorial experiment in which *Mesodinium chamaeleon* were acclimated to four different prey types (abbreviated CM, HP, RS, and SM) and exposed to three different light levels (10, 50, or 100  $\mu\text{mol quanta} \cdot \text{m}^{-2} \cdot \text{s}^{-1}$ ) while being either starved or fed. In fed trials, *M. chamaeleon* were offered prey at an initial ratio of 10 prey cells to 1 *M. chamaeleon* cell, which is within the linear portion of the saturating predator-prey (Holling Type II) functional response (Holling 1959, Moeller and Johnson 2018). All experiments began with an initial culture volume of 70 mL, containing 500 *M. chamaeleon* cells  $\cdot \text{mL}^{-1}$  (and 5,000 prey cells  $\cdot \text{mL}^{-1}$  in fed trials). All experiments (3 light levels  $\times$  4 prey types  $\times$  2 feeding regimes = 24 experiments) were run in triplicate in 70mL single-use tissue culture flasks (Part number 353082, Falcon Brand, Corning Inc., Corning, NY, USA).

Each experiment ran for 2 weeks, with sampling timepoints on days 0, 1, 2, 4, 6, 8, 10, 12, and 14. At each sampling timepoint, three types of measurements were made. (1) *Cell enumeration:* 1 mL of culture volume was preserved in a final concentration of 1% Acid Lugol's Solution, and *Mesodinium chamaeleon* (and prey, if present) were counted on an Axio Scope A1 compound microscope (Carl Zeiss Microscopy, LLC, Thornwood, NY, USA) at a magnification of 100x under

bright-field illumination. (2) *Photophysiology*: Fluorescence-based photosynthesis-irradiance curves, photosynthetic efficiency, and chlorophyll content were assayed, as described below. (3) *Plastid enumeration*: *M. chamaeleon* cells were filtered onto 0.8  $\mu\text{m}$  25 mm diameter polycarbonate filters (type HTTP, EMD Millipore, Darmstadt, Germany) and frozen at  $-20^{\circ}\text{C}$  for later DNA extraction and quantitative PCR analysis (see below). In fed cultures, it was necessary to wash cells free of prey prior to the latter two measurements. This was done using gravity filtration: Culture aliquots were placed onto 8.0  $\mu\text{m}$  transwell filters in 6-well tissue culture plates, which retained the ciliates while prey were washed away using 50 mL of filtered seawater (Peltomaa and Johnson 2017, Moeller and Johnson 2018).

To determine ingestion rates and measure prey photophysiology baselines, we also ran predator-free control experiments in which only prey were inoculated (at concentrations of 5,000 prey cells  $\cdot\text{mL}^{-1}$ ) into 70 mL of filtered seawater. These experiments were sampled in the same manner as the *Mesodinium chamaeleon* experiments.

*Photophysiology measurements*. We used fluorescence-based methods to determine photosynthetic capacity (Gorbunov et al. 1999) using a mini Fluorescence Induction and Relaxation (FIRe) system (custom built by M. Gorbunov, Rutgers University, New Brunswick, NJ, USA). After dark-acclimating cells for at least 15 min, we measured photosynthetic efficiency (Fv/Fm) as the ratio of photosynthetically active photosystems to total photosystems, and then generated photosynthesis-irradiance curves by measuring electron transport at twenty light levels spaced between 0 and 500  $\mu\text{mol quanta} \cdot \text{m}^{-2} \cdot \text{s}^{-1}$ . Using non-linear least squares regression (base R function *nls*), we fit these data to the phenomenological photosynthesis-irradiance equation of Jassby and Platt (1976):

$$\text{ETR} = P_{\max} \cdot \tanh\left(\frac{\alpha \cdot I}{P_{\max}}\right)$$

where  $P_{\max}$  is the maximum electron transport rate,  $\alpha$  is the initial slope of ETR with respect to light, and  $I$  is the incident irradiance. This fitting and all other calculations were performed using the software package R (R Core Team 2014). We compared means across treatment groups using analysis of variance (ANOVA) tests corrected for multiple hypothesis testing with Tukey's Honestly Significant Difference (HSD) tests. Data and analysis files are available at <https://doi.org/10.5281/zenodo.4361739>.

We converted electron transport rates (electrons per chlorophyll-*a* per second) to carbon fixation rates by assuming a quantum yield of oxygen evolution of 0.25 (4 electrons needed per molecule of  $\text{O}_2$ ) and a photosynthetic quotient of 1.4 ( $\text{O}_2$  produced per  $\text{CO}_2$  fixed; Laws 1991, Lawrenz et al. 2013). To convert from per-chlorophyll carbon fixation rates to cellular carbon fixation rates, we multiplied by cellular chlorophyll-*a* content.

Cellular chlorophyll-*a* (chl-*a*) content was measured by filtering live cells onto a 25 mm diameter GF/F filter (Whatman) and extracting for 24 h in a 90% acetone solution. Chl-*a* concentration in the acetone solution was read using a Trilogy fluorometer with a 460 nm LED (Turner Designs, San Jose, CA, USA). We computed the net decay rate of chl-*a* in *Mesodinium chamaeleon* in the same manner that one would compute a growth (loss) rate: as the slope of a line fit through the natural log of chl-*a* content over time. Here, we computed loss rates over the first 6 d of starved experiments only (because feeding results in the acquisition of new prey chlorophyll). Mean chl-*a* residence time was computed as the inverse of the loss rate.

To conservatively contrast kleptoplastid performance in *Mesodinium chamaeleon* relative to its prey, we computed maximum performance (e.g., maximum Fv/Fm, chl-*a*, and photosynthetic rates) for fed *M. chamaeleon* cells only. Even well-fed *M. chamaeleon* cells likely contain kleptoplastids of a variety of ages because kleptoplastids can be retained for days or even weeks, *sensu* Moeller and Johnson (2018). However, in our view measures of maximum performance represent the highest potential performance for kleptoplastids. Thus, focusing on maximum performance allowed us to conservatively estimate decreases in kleptoplastid function in the ciliate relative to the cryptophyte prey.

*Plastid enumeration*. We used a phenol-chloroform extraction to extract DNA from *Mesodinium chamaeleon* (Gast et al. 2004, Moeller and Johnson 2018), followed by qPCR to enumerate ciliates (targeting the nuclear small subunit rRNA (18S) gene) and plastids (targeting the plastid-encoded large subunit of RuBisCO (*rbL*) gene). We used primers (synthesized by Integrated DNA Technologies, Coralville, IA, USA) and annealing temperatures designed to target each cryptophyte (Table 1). Standard curves for each species were prepared by collecting triplicate dilution series containing 200, 1,000, 2,000, 10,000, 20,000, 100,000, and 200,000 cryptophyte cells (or 50, 500, 1,000, 5,000, and 10,000 *M. chamaeleon* cells). Dilution series cell concentrations were verified through cell fixation and microscopy counts (see above). All qPCR assays were conducted using a CFX96 Real-Time PCR detection system (Bio-Rad, Hercules, CA, USA) with SsoFast EvaGreen Supermix (Bio-Rad; reaction volume: 20  $\mu\text{L}$ ) and reaction conditions as described in Peltomaa and Johnson (2017).

*Growth and ingestion*. We calculated *Mesodinium chamaeleon* initial growth rate as the slope of a line fit through the natural log of population size over time (base R function *lm*). Because ciliate growth rates were typically sustained only for the first 4–6 d of the experiment, we computed growth rates over a 96 (starved experiments, in which growth was more limited) to 144-h (fed experiments) window. We also computed the extent of *M. chamaeleon* growth as the fold increase in population over the course of the 14-d experiment. That is, growth extent = (maximum *M. chamaeleon* population size)/(initial *M. chamaeleon* population size). Growth extent is a measure of yield or the average number of daughter cells produced by a single initial *M. chamaeleon* cell over the course of the 14-d experiment.

We computed ingestion using the method of Jeong and Latz (1994), in which growth rates of predator-free controls are compared with prey growth (or loss) rates in experiments. The difference in these rates is the grazing rate; normalizing to *Mesodinium chamaeleon* abundance gives an ingestion rate (Jeong and Latz 1994). Ingestion rates were computed using the first 48 h of data for all experiments to minimize flask effects.

*Cellular carbon content*. In order to normalize data to cellular carbon content, we conducted a second, smaller experiment in which we acclimated *Mesodinium chamaeleon* to each of the four prey types for a period of 6 weeks at a light level of 10  $\mu\text{mol quanta} \cdot \text{m}^{-2} \cdot \text{s}^{-1}$  (the lowest light level used in our full experiment). We grew well-fed cultures (fed every 3 d at a cryptophyte:*M. chamaeleon* ratio of at least 5:1) in triplicate to a concentration of 3,000–5,000 cells  $\cdot\text{mL}^{-1}$ , enumerated cultures using Lugol's fixation and microscopy counts (described above) and then filtered 10 mL of culture onto a pre-combusted GF/F filter (Whatman Cytiva, Marlborough, MA, USA). Total carbon was measured on an elemental analyzer (Model CEC 440HA, Control Equipment Corp., North Chelmsford, MA, USA). We also collected cellular carbon data on the cryptophyte prey at 10  $\mu\text{mol quanta} \cdot \text{m}^{-2} \cdot \text{s}^{-1}$ ,

TABLE 1. Primers used for quantitative PCR assays and their annealing temperatures.

Primer	Sequence	Temp. (°C)
<i>Chroomonas mesostigmatica</i> CM_rbcL_F	5' GCTGCTGCTGCTGGTGAAG 3'	63.2
<i>Chroomonas mesostigmatica</i> CM_rbcL_R	5' TTTACGTGCCCAGATACCCATAGA 3'	
<i>Hemiselmis pacifica</i> HP_660F	5' TGGTGCTAGTGCTGGTGA 3'	58.5
<i>Hemiselmis pacifica</i> HP_750R	5' ACAAATTACAGAACCTAAATCAGAAC 3'	
<i>Storeatula major</i> SM_rbcL_F2*	5' GATTAAGGTCACTACTTCAACATTACT 3'	60.0
<i>Storeatula major</i> SM_rbcL_R2*	5' GTAAGATCATACTGTTCTTACGAGC 3'	
<i>Mesodinium chamaeleon</i> MC_1640F	5' TGGAGGTGTGGGGTGCT 3'	63.0
<i>Mesodinium chamaeleon</i> MC_1830R	5' AGGGATGTTTTGGAGCGTGA 3'	

\*These primers were also used for *Rhodomonas salina* with an annealing temperature of 58.3°C.

using 10 mL of culture at 20,000 to 50,000 cells · mL<sup>-1</sup> (with exact concentrations determined through Lugol's fixation and microscopy counts, described above).

*Quantifying heterotrophic and photosynthetic contributions to growth.* We used our time series data to compute the total prey consumed, and total carbon fixed, per initial *Mesodinium chamaeleon* cell in each experimental replicate. To compute total prey consumption, we first calculated the total prey ingested as

$$\text{Total Prey Ingested} = \int_{t=0}^{14 \text{ d}} (g \cdot \text{Prey}) dt$$

where  $g$  is the grazing rate (per day), and prey abundances were measured in cells · mL<sup>-1</sup>. Because our experimental timepoints were coarse (every 2 d from day 2 to day 14), we approximated this integral using trapezoidal integration (R function *trapz* in package *pracma*). We divided this total ingestion by the initial *M. chamaeleon* abundance (in cells/mL) to determine a metric of prey consumption attributable to a single initial ciliate cell. We also computed total prey ingested in units of carbon by multiplying by prey cellular carbon content and dividing by *M. chamaeleon* cellular carbon content.

To compute total carbon fixed, we used trapezoidal integration to compute

$$\text{Total Carbon Fixed} = \int_{t=0}^{14 \text{ d}} (P_{\text{chl}}(I) \cdot \text{chl}_{\text{cell}}) dt$$

where  $P_{\text{chl}}(I)$  was the time-varying chlorophyll-specific carbon fixation rate at the growth irradiance  $I$ , and  $\text{chl}_{\text{cell}}$  was the time-varying chlorophyll content of each *Mesodinium chamaeleon* cell. As with prey consumption, we divided this total carbon fixation by the initial *M. chamaeleon* abundance (at  $t = 0$ ) to determine the carbon fixation attributable to a single initial cell. We also normalized photosynthetic yield to units of cellular carbon by dividing by *M. chamaeleon* cellular carbon content.

## RESULTS

*Mesodinium chamaeleon retains functional plastids from all four prey types.* Our starvation experiment revealed that functional prey plastids are retained for at least 14 d by *Mesodinium chamaeleon* (Fig. 1; Figs. S1–S8 in the Supporting Information show full data timeseries). Light-driven electron transport was maintained (Fig. 1A), and by day 14, all starved *M.*

*chamaeleon* were still capable of photosynthetic carbon fixation (Fig. 1B). These photosynthetic rates ranged from 0.5 g C · g chl- $a^{-1}$  · h<sup>-1</sup> at the lowest light level, to 8 g C · g chl- $a^{-1}$  · h<sup>-1</sup> at the highest light level. Photosynthetic efficiency (Fv/Fm) declined by as much as 75% for *Chroomonas mesostigmatica*-fed *M. chamaeleon* at the highest light levels (Fig. 1C). Declines in photosynthetic efficiency were lowest (~40%) for red plastids, though the rate of chlorophyll- $a$  loss was higher for *M. chamaeleon* with red plastids (Fig. 1D). Generally, chlorophyll- $a$  loss rate increased with increasing light (Fig. 1D), except for *Storeatula major*-fed *M. chamaeleon*.

The mechanism of loss of photosynthetic capacity varied by prey type and light level. The sensitivity of the photosystem to light ( $\alpha^B$ , the chl- $a$  normalized initial slope of the photosynthesis-irradiance curve) decreased at low light levels, but increased at the highest light level for red plastid types (Fig. 1E). Over time, the maximum per-chlorophyll- $a$  electron transport rates ( $P_{\text{max,ETR}}$ ) of blue-green kleptoplastids tended to increase, while these rates declined in red kleptoplastids (Fig. 1F, Fig. S9 in the Supporting Information). These declines were more pronounced in low-light environments. Thus, *M. chamaeleon* that retained blue-green plastids were able to sustain a high percentage of their original (Day 0) carbon fixation rates over the course of 2 weeks of starvation (Fig. S10 in the Supporting Information). In contrast, although carbon fixation rates were initially higher for *M. chamaeleon* with red plastids, these rates fell precipitously by the end of the experiment (Fig. S10) due to a combination of declines in photosystem performance (Fig. 1F, Fig. S9) and loss of photosynthetic pigment (Fig. 1D).

Photosystem-for-photosystem, plastids generally performed better in their original hosts (cryptophytes) than as kleptoplastids hosted by *Mesodinium chamaeleon* (Fig. 2, Fig. S11 in the Supporting Information). Except for *Rhodomonas salina* at the highest light level, photosynthetic efficiencies were always higher in cryptophytes than in *M. chamaeleon* (Fig. 2A). As light level increased, so too did the marginal improvement in plastid performance in the native cryptophyte host. Both maximum per-chlorophyll photosynthetic rate (Fig. 2B) and photosynthetic rate at the growth

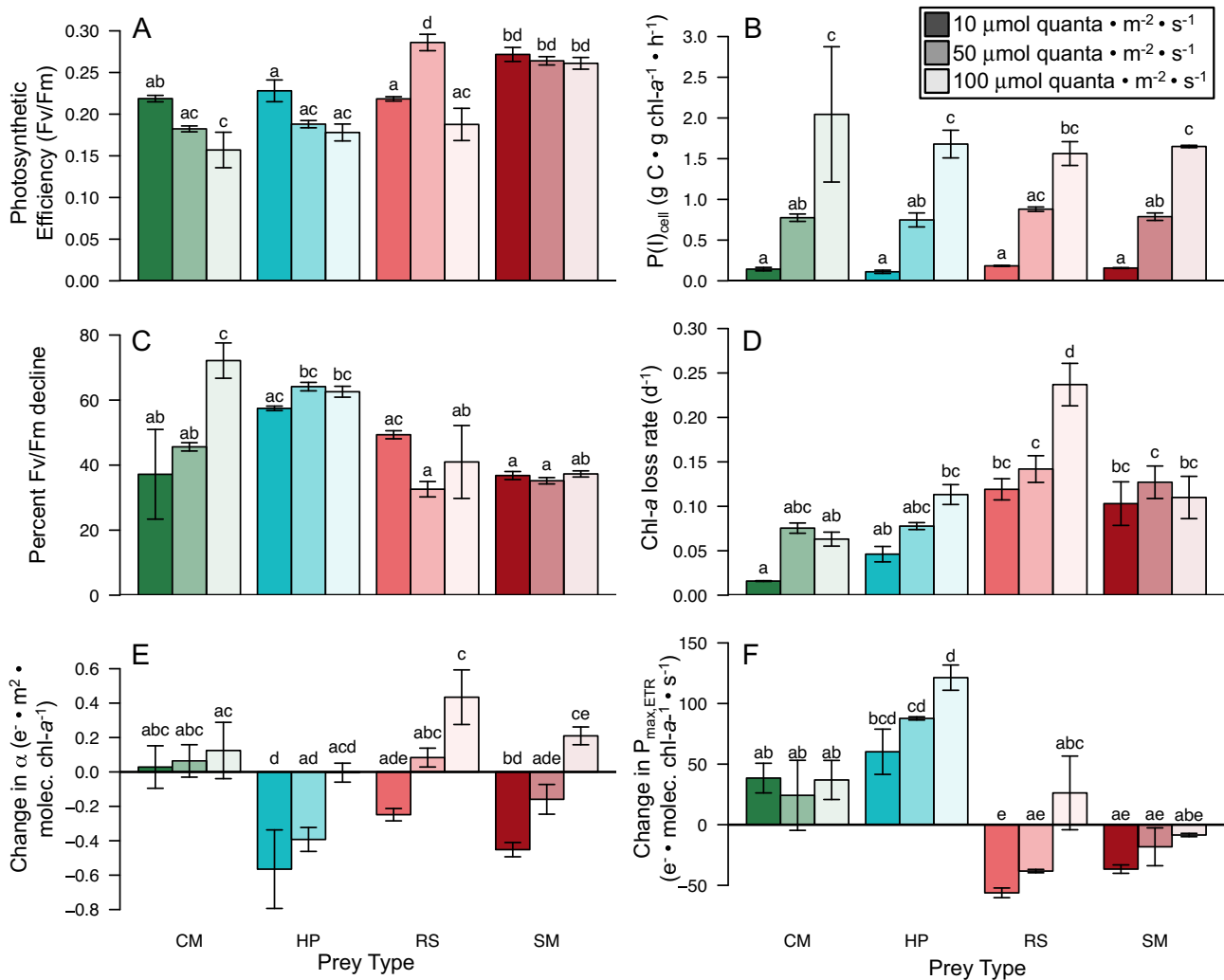


FIG. 1. Maintenance of photosynthetic capacity in starved *Mesodinium chamaeleon* over 14 d of starvation. A: *M. chamaeleon* fed all four prey types maintained photosynthetic capacity, with Fv/Fm measurements indicating that 15–25% of photosystems were still competent for electron transfer. B: Sufficient (active) pigment remained to support photosynthetic fixation of carbon at rates of up to  $8 \text{ g C} \cdot (\text{g chl-}a)^{-1} \cdot \text{h}^{-1}$ . C: Photosynthetic efficiency declined for all prey types, with the highest losses in photosynthetic capacity occurring for blue-green plastids (*Chroomonas mesostigmatica* and *Hemiselmis pacifica*) at high light levels. D: Chlorophyll-*a* content also declined over time, with rates of pigment loss generally increasing with light (except for *Storeatula major*). E: Except for *M. chamaeleon* containing *C. mesostigmatica* plastids, changes in  $\alpha^B$  (the initial slope of the photosynthesis-irradiance curve and representative of light sensitivity) were negative (representing a decrease in  $\alpha^B$  over the 14-d starvation period) in low light and zero or positive (representing an increase in  $\alpha^B$  over the 14-d starvation period) at high light. F:  $P_{\text{max}}$  (also normalized to chlorophyll-*a*) tended to increase during starvation for blue-green plastid types, but decreased at low light for red plastid types. Data are all from starved cultures. Bar heights represent means, and whiskers represent  $\pm$  one standard error across three replicates. Letters represent statistically significant differences (Tukey's HSD,  $P < 0.05$ ). [Colour figure can be viewed at [wileyonlinelibrary.com](http://wileyonlinelibrary.com)]

irradiance (Fig. 2D) increased with light more strongly in the cryptophyte than in *M. chamaeleon*. As a consequence, although *M. chamaeleon* cells contained as many as 30 plastids  $\cdot \text{cell}^{-1}$  (Fig. 3A) and, on average, roughly ten times the amount of chlorophyll-*a* as their cryptophyte prey (Fig. 3B), per-cell carbon fixation rates were only fivefold higher than those of cryptophytes (Fig. 3C). When normalized to cellular carbon (Fig. S12 in the Supporting Information), pigment content was more similar between *M. chamaeleon* and its prey (Fig. 3D), but photosynthetic rates were twice as high in cryptophytes as in *M. chamaeleon* (Fig. 3E).

While prey cells exhibited strong evidence of their capacity for photoacclimation (decreased chl-*a* and photosynthetic efficiency, but increasing carbon fixation, with increasing light), evidence for photoacclimatory capacity in *Mesodinium chamaeleon* was more equivocal (Figs. 2, 3). For example, while per-cell chlorophyll content tended to decrease with increasing light, this decrease was not always monotonic (Fig. 3B). Trends in photosynthetic efficiency were also less apparent, with kleptoplastids from *Hemiselmis pacifica* showing the only clear monotonic decline (Fig. 3B). Overall, patterns in pigment

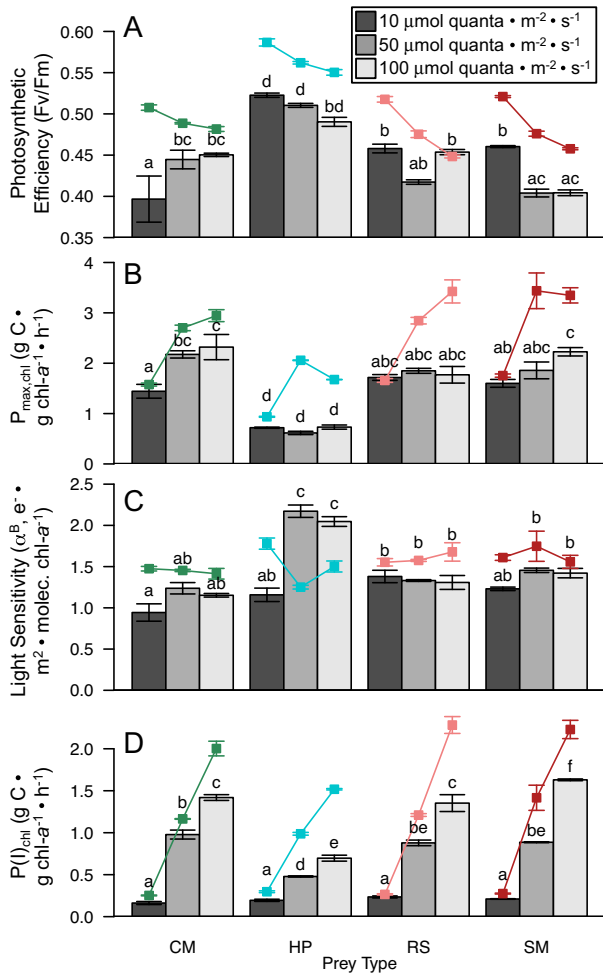


FIG. 2. *Mesodinium chamaeleon* photophysiology (bar graphs) relative to cryptophyte prey (filled points and lines). A: *M. chamaeleon* had lower photosynthetic efficiency for all but one prey  $\times$  light combination. Unlike free-living cryptophytes, which displayed the canonical photoacclimation response of decreasing photosynthetic efficiency with increasing light, *M. chamaeleon* photosynthetic efficiencies decreased with light only when bearing *Storeatula major* plastids. B: Except at the lowest light levels, *M. chamaeleon* maximum carbon fixation rates ( $P_{\max,chl}$ ) were lower than free-living prey. These maximum rates increased with light for all prey except *Hemiselmis pacifica*, but were generally light-insensitive in *M. chamaeleon*. C: Light sensitivity ( $\alpha^B$ ) tended to be insensitive to light and more similar across *M. chamaeleon* and its plastid source, except in the case of *H. pacifica*, where *M. chamaeleon* had greater  $\alpha^B$ . D: While all organisms photosynthesized at greater rates with increasing growth irradiance, when normalized to chl-*a* ( $P(I)_{chl}$ ), free-living cryptophyte performance outstripped that of *M. chamaeleon* at higher light levels. Bar heights (or, for free-living cryptophytes, square symbols) represent means, and error bars represent  $\pm$  one standard error. Letters represent statistically significant differences (Tukey's HSD,  $P < 0.05$ ). [Colour figure can be viewed at [wileyonlinelibrary.com](http://wileyonlinelibrary.com)]

content and photosynthetic performance in *M. chamaeleon* tended to mirror those of its prey, albeit at lower magnitudes. For example, chl-*a* content was highest in *M. chamaeleon* fed the phycoerythrin-bearing cryptophytes *Rhodomonas salina* and *Storeatula major*, which had the highest cellular chl-*a* content

themselves (Fig. 3B). And although *H. pacifica* plastids had some of the highest photosynthetic efficiencies (Fig. 2A), per-cell carbon fixation rates were lowest in both *H. pacifica* cryptophytes, and in *M. chamaeleon* acclimated to this prey species (Fig. 3C).

*Mixotrophic, but not phototrophic, growth of Mesodinium chamaeleon increased with light.* *Mesodinium chamaeleon* grew faster (Fig. 4, A–D) and to a greater extent (Fig. 4, E–H) when fed. Mixotrophic (but not solely photosynthetic) growth rates increased with increasing light (Fig. 4, A–D). That is, *M. chamaeleon* growth rates increased with light availability only when prey were present. This growth response to light mirrored that of its prey, which, with the exception of *Hemiselmis pacifica*, also grew faster with increasing light. When fed at high light ( $100 \mu\text{mol quanta} \cdot \text{m}^{-2} \cdot \text{s}^{-1}$ ), *M. chamaeleon* was capable of achieving its highest growth rates ( $\sim 0.6 \cdot \text{d}^{-1}$ ) regardless of prey type, but when starved growth rates were more constant ( $\sim 0.2 \cdot \text{d}^{-1}$ ), except in the case of *Chroomonas mesostigmatica*, in which *M. chamaeleon* exhibited very low or even negative growth rates when starved of prey at high light. The extent of photosynthetic growth did not differ with light (Fig. 4, E–H, black bars), but the extent of mixotrophic growth by *M. chamaeleon* fed *C. mesostigmatica* or *Rhodomonas salina* did increase as light levels increased (Fig. 4, E and G, gray bars).

While *Mesodinium chamaeleon* yield tended to be more extensive when growth rates were highest (black line, Fig. 4I), these relationships differed by prey species (colored lines, Fig. 4I). For example, although *M. chamaeleon* fed *Hemiselmis pacifica* at high light grew at some of the highest rates, this growth was limited in its extent with populations at best quadrupling over the course of the experiment. In contrast, *M. chamaeleon* acclimated to *Rhodomonas salina* achieved similar growth rates, but grew for a longer period of time, exhibiting up to a 12-fold increase when fed (7-fold when starved).

*Both feeding and increased photosynthetic rates supported mixotrophic growth.* *Mesodinium chamaeleon* ingested prey of all types at all light levels, and feeding was correlated with mixotrophic growth. With the exception of *Rhodomonas salina*, ingestion rates increased with light, to a maximum of  $\sim 15$  prey cells ingested  $\cdot M. chamaeleon^{-1} \cdot \text{d}^{-1}$  (Fig. 5A). Across the experiment, higher ingestion rates were correlated with higher growth rates (Fig. 5B, black line), although within prey type, this trend held only for *Hemiselmis pacifica* and *Storeatula major* (Fig. 5B, blue and red lines, respectively) due to greater contributions from photosynthesis to growth at high light. Cumulative prey ingestion (integrated across the 14-d experiment) was greatest for *M. chamaeleon* fed *C. mesostigmatica* at 50 and  $100 \mu\text{mol quanta} \cdot \text{m}^{-2} \cdot \text{s}^{-1}$  light levels (Fig. 5C). This higher ingestion occurred because elevated prey growth rates (Fig. 4A) allowed persistence of CM prey over a longer period of time than in other fed

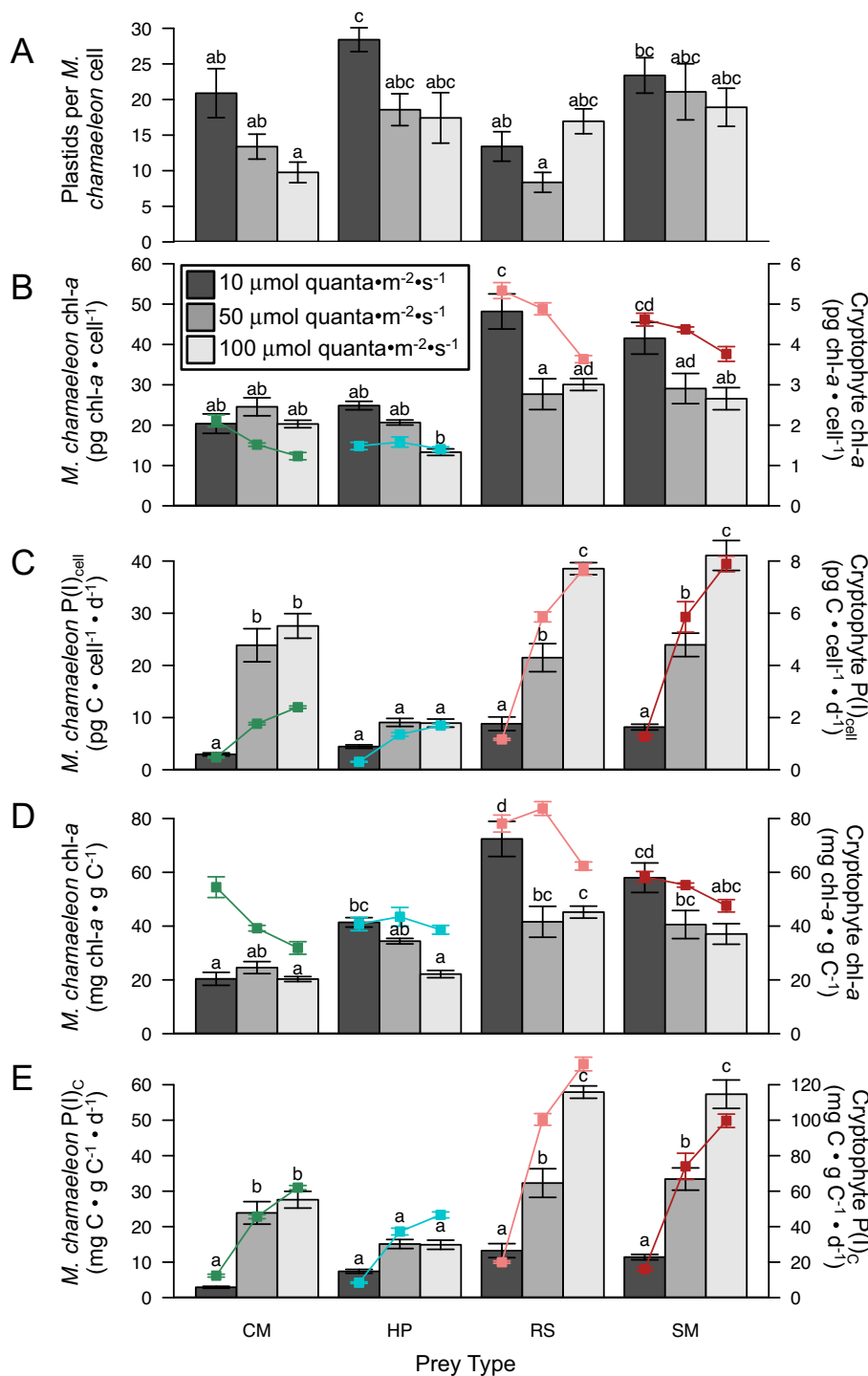


FIG. 3. Variation in photosynthetic machinery content across prey and light treatments. A: Maximum plastid counts varied by light and prey type, and were lowest for *Mesodinium chamaeleon* fed *Chroomonas mesostigmatica* in high light. B: *M. chamaeleon* cells (bars) typically contained an order of magnitude more chlorophyll-*a* than their cryptophyte prey (points, note different y-axis scales), and cells containing blue-green plastids had lower chl-*a* content than those with red plastids. While cryptophytes exhibited evidence for photoacclimation (chl-*a* content decreased with light), this pattern was absent in *M. chamaeleon* fed *C. mesostigmatica* and equivocal for other prey types. C: Photosynthesis rates (presented here in units of  $\text{pg C}_{\text{fixed}} \cdot \text{C}^{-1} \cdot \text{h}^{-1}$ ) were roughly five times greater in *M. chamaeleon* than in prey cells, and mirrored prey increases with increasing light availability. D: When normalized to cellular C, pigment content was more similar (note same y-axis scales). E: When photosynthesis rates were normalized to carbon, cryptophytes outperformed *M. chamaeleon* by a factor of 2. Bar heights (or, for cryptophyte measures, square symbols) represent means, and error bars represent  $\pm$  one standard error. Letters represent statistically significant differences (Tukey's HSD,  $P < 0.05$ ). [Colour figure can be viewed at [wileyonlinelibrary.com](http://wileyonlinelibrary.com)]

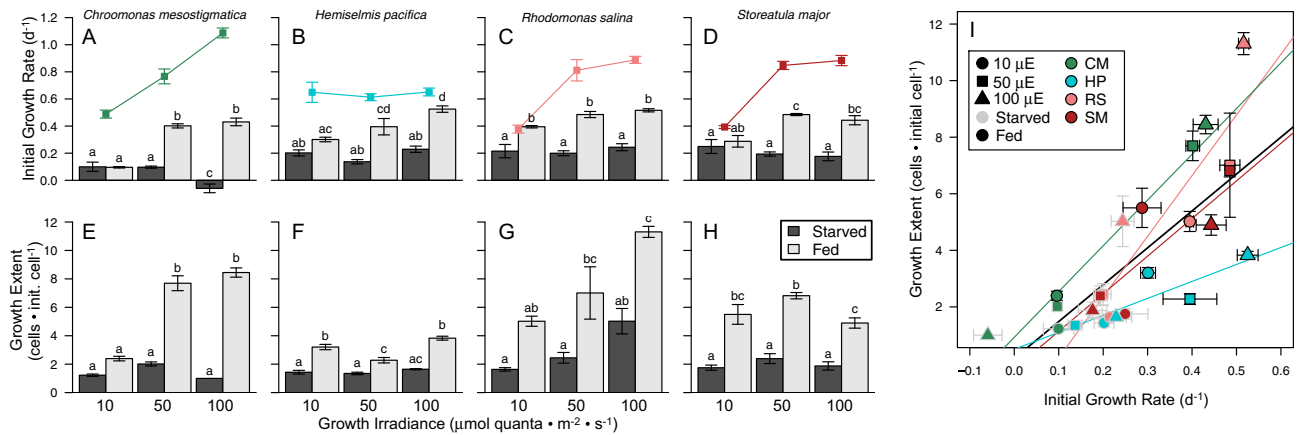


FIG. 4. Effects of prey type, light, and feeding on *Mesodinium chamaeleon* growth rate and extent. A–D: *M. chamaeleon* growth rates were generally higher for fed (light gray bars) as opposed to starved (dark gray bars) cells. For fed cells, growth rates increased with light ( $x$ -axis), mirroring trends observed in prey (colored lines). E–H: The extent of growth, measured as the maximum increase in *M. chamaeleon* relative to initial population size over the course of the 14-day experiment, was also greatest for fed cells. *M. chamaeleon* exhibited more sustained growth when fed *Rhodomonas salina*, although it achieved similar growth rates when offered the other cryptophyte types. Bar heights (or, for cryptophyte growth rates, square symbols) represent means, and error bars represent  $\pm$  one standard error. Letters represent statistically significant differences (Tukey's HSD,  $P < 0.05$ ). I: While rapid growth was necessary for sustained growth, not all rapidly growing *M. chamaeleon* continued to grow through numerous cell divisions. The highest growth rates and extents were achieved by fed cells. Point colors represent prey types, shapes represent light levels, and line shading indicates whether *M. chamaeleon* were starved (gray) or fed (black). Error bars show  $\pm$  one standard error around the mean value for each experimental treatment. Where present, lines indicate a significant ( $P < 0.001$ ) correlation across the experiment (black line; linear model:  $F_{70} = 86.4$ ,  $R^2 = 0.546$ , residual standard error (RSE) = 1.892) or within a treatment group (green: *Chroomonas mesostigmatica*,  $F_{16} = 138.7$ ,  $R^2 = 0.890$ , RSE = 1.054; teal: *Hemiselmisa pacifica*,  $F_{16} = 45.33$ ,  $R^2 = 0.723$ , RSE = 0.5175; salmon: *R. salina*,  $F_{16} = 39.13$ ,  $R^2 = 0.692$ , RSE = 1.951; red: *Storeatula major*,  $F_{16} = 36.33$ ,  $R^2 = 0.675$ , RSE = 1.194).

treatments (Fig. S1). Thus, while higher cumulative prey consumption correlated with more extensive growth across the experiment (Fig. 5D, black line), this trend was driven by *C. mesostigmatica*-fed *M. chamaeleon* (Fig. 5D, green line).

Feeding also increased *Mesodinium chamaeleon* photosynthetic activity, leading to more growth (Fig. 6). Fed cells fixed more carbon over the course of the 14-d experiment (Fig. 6, A–D), with feeding resulting in total carbon fixation amounts that were sometimes as much as 18-fold greater than those observed in starved cells (Fig. 6E). *Mesodinium chamaeleon* accumulated more carbon per ingested prey for red plastids, especially those of *Rhodomonas salina*, with carbon fixation amounts of up to 2.5 pg C per prey cell ingested (Fig. 6F). The more cells photosynthesized, the more they grew (Fig. 6G). Cumulative photosynthetic activity (total carbon fixed over the entire 14-d experiment) was a good predictor of growth extent (Fig. 6G, black line), especially for fed treatments and starved *R. salina*-acclimated *M. chamaeleon* (Fig. 6G, colored lines).

#### DISCUSSION

Kleptoplastidic lineages retain functional plastids from their photosynthetic prey, but the efficiency and duration with which they retain these plastids vary with host and prey type. In this study, we assessed how a single host species (the marine

ciliate *Mesodinium chamaeleon*) used plastids from four genera of prey for photosynthesis. Consistent with field observations and previous studies, we found that plastids could be retained from all four prey types (Moeller and Johnson 2018, Kim and Park 2019). However, plastid function and, as a consequence, ciliate growth, varied. Contrary to our overarching hypothesis that phycocyanin-containing plastids would support the greatest growth in *M. chamaeleon*, our data suggest that the phycoerythrin-bearing cryptophytes *Rhodomonas salina* and *Storeatula major* supported the greatest mixotrophic growth of *M. chamaeleon* (Fig. 4). In contrast, while *M. chamaeleon* cells acclimated to phycocyanin-bearing prey maintained photosynthetic capacity (Fig. 1) and even increased maximum photosynthetic rate (Fig. S9), they had sharply decreased (and even negative) growth rates under starvation (i.e., *Chroomonas mesostigmatica*) and limited growth extents even when well-fed (i.e., *Hemiselmis pacifica*). However, field observations of *M. chamaeleon* (including our own, when this culture was first isolated) and the functionally similar sister-species *M. coatsi* suggest that blue-green plastids are more common in nature (Moestrup et al. 2012, Moeller and Johnson 2018, Kim and Park 2019).

There are several possible explanations for this apparent contradiction: First, our testing of prey types was not comprehensive, so the blue-green plastids *Mesodinium chamaeleon* obtains in nature may

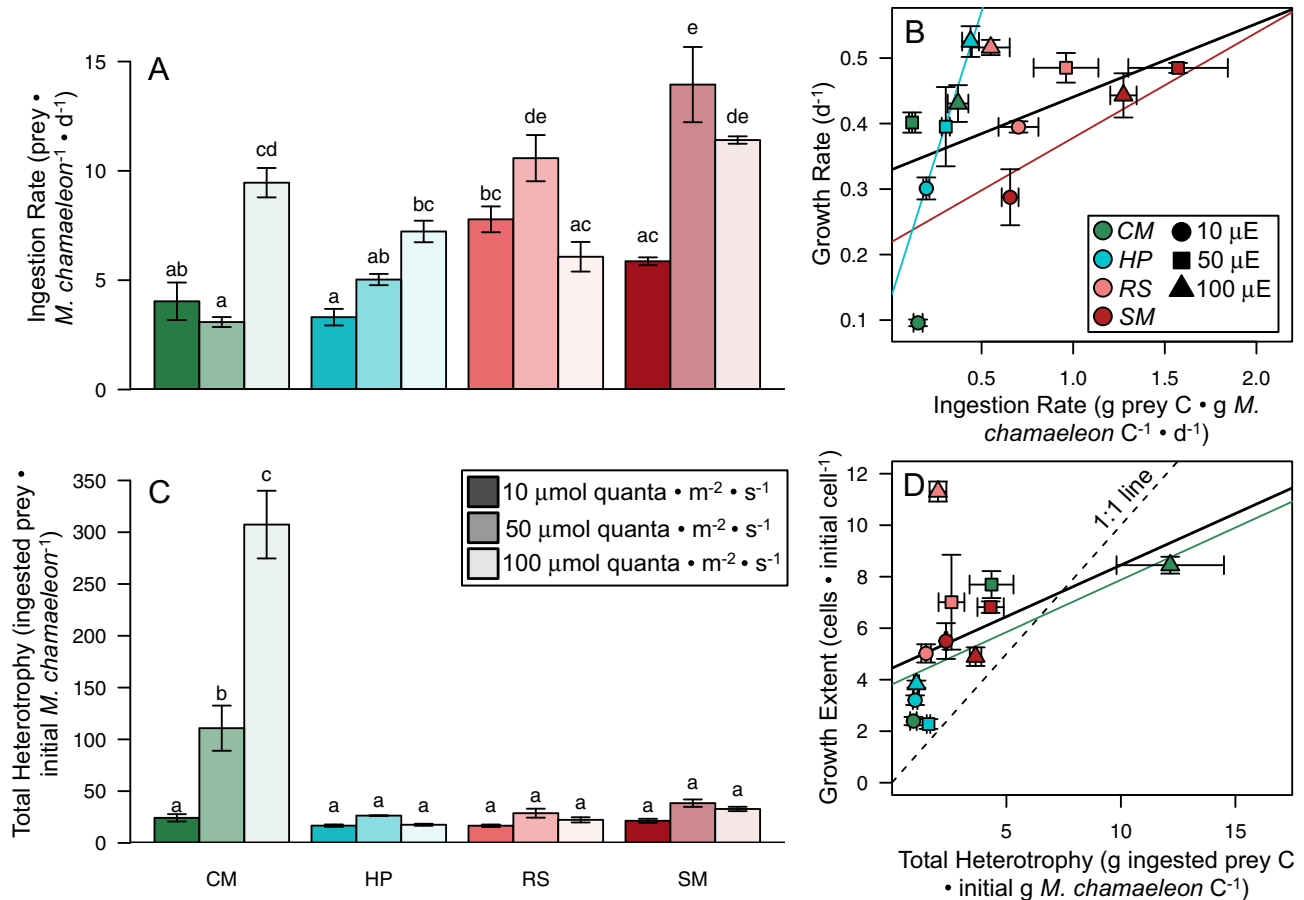


FIG. 5. Feeding and impact on *Mesodinium chamaeleon* growth. A: Ingestion rates varied across light level and prey type, with the highest ingestion rates observed for *Storeatula major* at light levels of  $50 \mu\text{mol quanta} \cdot \text{m}^{-2} \cdot \text{s}^{-1}$  or greater. Bar heights represent means, and error bars show  $\pm$  one standard error. Letters indicate significantly different means (Tukey's HSD,  $P < 0.05$ ). B: Across fed treatments, higher ingestion rates were correlated with faster *M. chamaeleon* growth rates (black line; linear model:  $F_{34} = 7.454$ ,  $P < 0.01$ ,  $R^2 = 0.156$ ,  $\text{RSE} = 0.1089$ ), but this trend was driven by data from *M. chamaeleon* fed *S. major* (red line; linear model:  $F_7 = 8.786$ ,  $P < 0.05$ ,  $R^2 = 0.493$ ,  $\text{RSE} = 0.06686$ ) or *Hemiselms pacifica* (blue line; linear model:  $F_7 = 27.53$ ,  $P < 0.005$ ,  $R^2 = 0.768$ ,  $\text{RSE} = 0.0593$ ). C: Total prey ingestion varied by treatment, with *M. chamaeleon* fed *Chroomonas mesostigmatica* at high levels eating the most prey of all treatments. D: Higher prey consumption (in g of prey C consumed per g C of initial *M. chamaeleon*) lead to more extensive growth (black line; linear model:  $F_{34} = 9.359$ ,  $P < 0.005$ ,  $R^2 = 0.193$ ,  $\text{RSE} = 2.483$ ), but this trend was driven entirely by *C. mesostigmatica* data (green line; linear model:  $F_7 = 9.52$ ,  $P < 0.05$ ,  $R^2 = 0.516$ ,  $\text{RSE} = 2.025$ ). Note that, except for *C. mesostigmatica*-fed *M. chamaeleon* at  $100 \mu\text{mol quanta} \cdot \text{m}^{-2} \cdot \text{s}^{-1}$ , the highest light level, the fold increase in *M. chamaeleon* exceeded what would be expected from heterotrophy alone (compare points to the dashed 1:1 line).

come from different sources than *Chroomonas mesostigmatica* or *Hemiselms pacifica* (Kim and Park 2019). Second, differences in prey availability likely shape the in situ plastid content of more diverse feeders like *M. chamaeleon*. Previous studies have shown that *M. chamaeleon* and *M. coatsi* plastids may turn over rapidly between prey types (Moeller and Johnson 2018, Kim et al. 2019), so field observations likely reflect a combination of prey availability and preference. *M. chamaeleon* and *M. coatsi* are found in benthic environments or in highly stratified pycnocline layers (Moeller and Johnson 2018, Kim et al. 2019), habitats that may select for blue-green cryptophytes such as *Chroomonas* (Kim et al. 2019). Third, prey types that produce maximal growth in a

laboratory setting may not be optimal under field conditions. Furthermore, organisms do not always display “optimal” behavior in the field.

While mixotrophs with permanent plastids—that is, “constitutive mixoplankton,” or “algae that eat” (Stoecker 1998, Flynn et al. 2019)—typically show a positive photosynthetic growth response (i.e., under starvation) to increasing light, in our study *Mesodinium chamaeleon*'s growth only was enhanced by light when prey were present. This reflects *M. chamaeleon*'s reliance on sustained access to stolen prey plastids to maintain photosynthetic capacity: Feeding provides both a direct (heterotrophic) and indirect (photosynthetic) source of carbon. In our study, we found no evidence that *M. chamaeleon* can

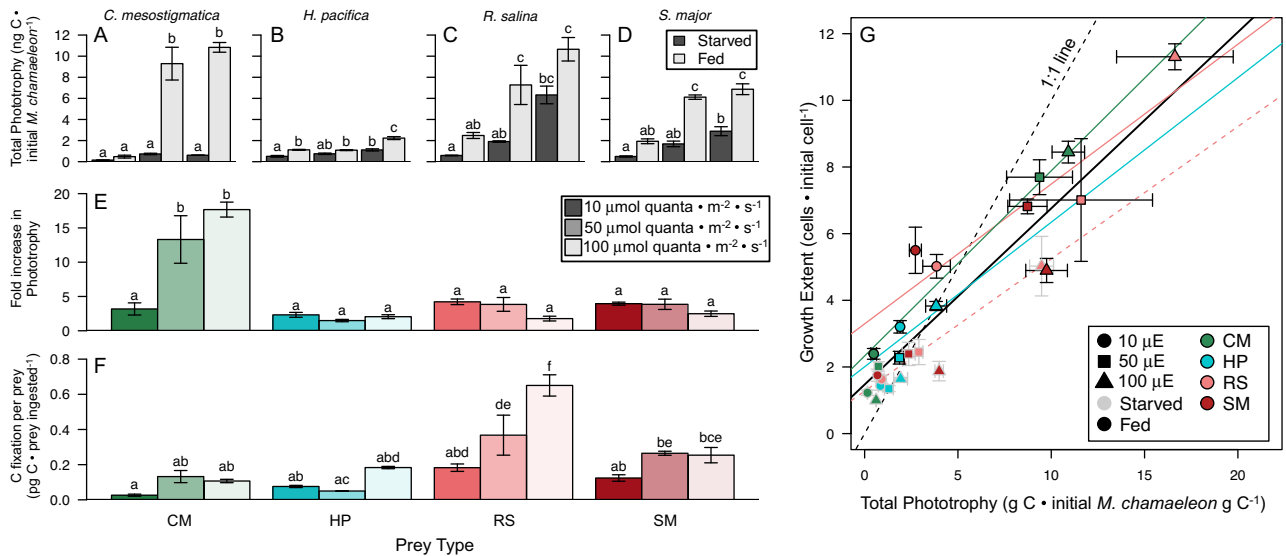


FIG. 6. Photosynthetic contributions to *Mesodinium chamaeleon* growth. A–D: Feeding enhanced total carbon fixation over the course of the 14-d experiment for all cell types (light gray bars). For all but *Chroomonas mesostigmatica*-acclimated starved *M. chamaeleon*, carbon fixation also increased with light. Bar heights represent means, and error bars represent  $\pm$  one standard error. Letters indicate significantly different means (Tukey's HSD,  $P < 0.05$ ). E: The effect of feeding varied by species. Except for *C. mesostigmatica*-fed cells at 50 and 100  $\mu\text{mol quanta} \cdot \text{m}^{-2} \cdot \text{s}^{-1}$ , total carbon fixation was 2–4 times higher in fed than starved cells. In *C. mesostigmatica*-fed treatments, however, gains were more pronounced—as high as 18-fold increases. F: The amount of carbon fixed per prey cell ingested was highest for red plastids, especially *Rhodomonas salina*. G: Higher carbon fixation lead to more extensive growth (black line; linear model:  $F_{70} = 310.2$ ,  $P < 0.001$ ,  $R^2 = 0.813$ ,  $\text{RSE} = 1.214$ ). Within prey treatments, this trend was observed *C. mesostigmatica* fed (green line; linear model:  $F_7 = 252.1$ ,  $P < 0.001$ ,  $R^2 = 0.969$ ,  $\text{RSE} = 0.5114$ ), *Hemiselembis pacifica* fed (blue line; linear model:  $F_7 = 5.713$ ,  $P < 0.05$ ,  $R^2 = 0.371$ ,  $\text{RSE} = 0.5743$ ), and *R. salina* fed (coral line; linear model:  $F_7 = 35.36$ ,  $P < 0.001$ ,  $R^2 = 0.811$ ,  $\text{RSE} = 1.408$ ) and starved (coral dashed line; linear model:  $F_7 = 26.89$ ,  $P < 0.005$ ,  $R^2 = 0.764$ ,  $\text{RSE} = 0.8509$ ) treatments. Note that in most cases (and especially for highly photosynthetic treatments), the fold increase in *M. chamaeleon* was lower than what would be expected from perfect incorporation of photosynthate into biomass (compare points to the dashed 1:1 line).

synthesize photosynthetic pigments: total chlorophyll-*a* monotonically declined for starved cells. This contrasts with our previous finding that *M. chamaeleon* fed *Storeatula major* may be capable of limited chl-*a* synthesis (Moeller and Johnson 2018). Because plastids and pigments degrade over time, *M. chamaeleon*'s photosynthetic capacity is tightly coupled to that of its prey and requires regular replenishment via prey ingestion. However, compared to plastidic oligotrichs, another major group of mixotrophic ciliates that retain plastids from diverse algal prey, sequestered plastids of *M. chamaeleon*, have greater longevity and function over time. Plastids in *M. chamaeleon* remained present and functional, even in starved cells after 2 weeks ( $\sim 10 \cdot \text{cell}^{-1}$ ), while plastidic oligotrichs appear to have a maximum retention time of 48–72 h (Schoener and McManus 2012). Comparisons between mixotrophs across different taxonomic groups are complicated by anatomical and functional traits that often vary dramatically, even among classes of ciliates. In the case of *M. chamaeleon*, the majority of prey organelles and cytoplasm are sequestered and maintained within distinct compartments, while oligotrichs only sequester plastids that may (Rogerson et al. 1989) or may not (Stoecker and Silver 1990) be maintained within a membrane compartment.

While comparisons among various mixotrophs are instructive for understanding the fundamental role of acquired phototrophy as an adaptive trait in shaping their ecology and evolution, they are most informative when comparing closely related taxa. When contrasted to *Mesodinium rubrum*, *M. chamaeleon* shares key similarities in feeding behavior, preference for cryptophytes, sequestration of most prey organelles, and sustained organelle maintenance. However, *M. rubrum* has greater prey specificity (Johnson et al. 2016, Peltomaa and Johnson 2017), organizes its stolen nucleus separate from plastid-organelle complexes (Gustafson et al. 2000, Johnson et al. 2006), and is capable of dividing plastids and synthesizing pigments (Johnson et al. 2006, Kim et al. 2017). Studies of the *Mesodinium* genus therefore provide a valuable opportunity for assessing the how acquired metabolism has modified trait selection and niche partitioning within these closely related species.

Because *Mesodinium chamaeleon* retains kleptoplasts from all four prey types used in this study, it is difficult to fully disentangle the relative contributions of heterotrophy and phototrophy to its growth. However, while across the entire experiment increased prey consumption and increased carbon fixation were linked with increased growth extent (Figs. 5D, 6C), some suggestive prey-specific patterns emerged. In particular,

the link between prey consumption and *M. chamaeleon* growth was driven by *Chroomonas mesostigmatica*-acclimated cells (Fig. 5D), while the link between phototrophy and growth was statistically significant for fed *C. mesostigmatica*-, *Hemiselmis pacifica*-, and *Rhodomonas salina*-acclimated *M. chamaeleon*, as well as for *R. salina*-acclimated starved *M. chamaeleon* (Fig. 6C). These findings imply that continuous replenishment (through grazing) of *C. mesostigmatica* plastids is necessary to sustain growth, whereas growth on *R. salina* is decoupled from grazing. The mechanisms underlying this differential plastid performance are unknown, although previous studies have found differences in plastid retention and growth in *M. chamaeleon* and *M. coatsi* (Moeller and Johnson 2018, Kim et al. 2019). While our study aimed at evaluating plastid performance by physiological traits manifested within *M. chamaeleon*, differences in intracellular signaling, surface proteins, and other factors may allow certain (i.e., *R. salina*) plastids to evade digestion. In contrast, *M. rubrum* only displays sustained growth when fed cryptophytes of the *Teleaulax/Plagioselmis/Geminigera* clade, although it will ingest other cryptophyte species (Park et al. 2007, Hansen et al. 2012). One Korean strain of *M. rubrum* has been shown, using PCR as evidence, to perhaps sequester plastids from a *Rhodomonas* sp. (strain CR-MAL03), although it cannot replace its *Teleaulax* plastids and shows only weak growth on CR-MAL03 (Myung et al. 2011).

Once ingested, plastid performance varied by cryptophyte origin. In part, this may be due to variation in the composition and photosynthetic capacity of phycobiliproteins found in each prey source (Cunningham et al. 2019, Greenwold et al. 2019). For example, the cryptophyte phycocyanin found in some *Chroomonas* species exhibit higher energy transfer efficiency than the cryptophyte phycoerythrin found in *Rhodomonas* species (Doust et al. 2006), which may contribute to observed elevated light capture in *Chroomonas* compared to *Rhodomonas* (Greenwold et al. 2019). We did not quantify phycobiliprotein content in cryptophytes or *Mesodinium chamaeleon* as part of our study, but previous work has shown that cryptophytes and *M. rubrum* down-regulate phycobiliprotein production in higher light environments (MacIntyre et al. 2002, Moeller et al. 2011, Deblois et al. 2013). Phycobiliprotein biosynthesis can also be decreased when nitrogen or phosphorus are limiting (Lewitus and Caron 1990). Thus, at high light levels and/or under low nutrient conditions, phycobiliproteins may have a lower impact on kleptoplastid light harvesting in *M. chamaeleon*. In previous work, we have seen no evidence for changes in *M. chamaeleon* growth as a function of nutrient amendment (Moeller and Johnson 2018). That is, unlike *M. rubrum*, *M. chamaeleon* does not grow more rapidly in nutrient-enriched media, suggesting it may lack the ability to take up and/or incorporate inorganic nutrients from the media. Future work could compare kleptoplastid pigment

and performance degradation in *M. chamaeleon* to that of free-living cryptophytes experiencing nutrient stress, to assess whether the ciliate cytoplasm resembles a nutrient-limited environment.

The extent of *Mesodinium chamaeleon* growth (fold increase) fell below the 1:1 line for photosynthesis (Fig. 6G), indicating either substantial respiratory costs or other inefficiencies in carbon assimilation from photosynthesis. However, the value of plastid retention is clear when the extent of growth is compared to carbon gained from heterotrophy (Fig. 5D): Except when feeding on *Chroomonas mesostigmatica* at the highest light level, fed *M. chamaeleon* grew more than would be predicted strictly from prey carbon ingested, even if this prey carbon were incorporated with 100% efficiency. We urge caution when interpreting these results, however, because our calculations are grounded in limited measurements of cellular carbon content from cells acclimated to the lowest light levels which, in the case of *M. chamaeleon*, were also well-fed. Cellular carbon content may vary with light level and feeding history (Moeller et al. 2011), so our calculation is likely less accurate at high light levels and in starved cultures.

Kleptoplastid performance may constrain *Mesodinium chamaeleon*'s location and abundance in coastal ecosystems. When feeding on prey whose kleptoplastid performance is similar to *Rhodomonas salina*, *M. chamaeleon* may be able to transiently decouple its growth from that of its prey (Moeller et al. 2016), but will need to feed more regularly than its sister-species *M. rubrum*, which can repair and even replicate prey plastids (Johnson et al. 2006, 2007). We also found some evidence (e.g., larger reductions in photosynthetic efficiency and faster pigment decay rates; Fig. 1) for more rapid degradation of photosynthetic machinery in higher light environments, likely because higher light increases the rate of photodamage (Long et al. 1994). *Mesodinium chamaeleon* and *M. coatsi* are typically found on or near the benthos (Nam et al. 2014, Kim and Park 2019, Kim et al. 2019), and our isolate came from a low light environment of less than  $5 \mu\text{mol quanta} \cdot \text{m}^{-2} \cdot \text{s}^{-1}$  (Moeller and Johnson 2018). While benthic habitats are not always low light, this localization may be an adaptive mechanism to decrease photooxidative stress and preserve plastid performance.

Mixotrophic growth may also allow for niche partitioning between *Mesodinium chamaeleon* and *M. coatsi*, and their more photosynthetic and strictly heterotrophic congeners. In this study, we did not offer *M. chamaeleon* prey known to be preferred by the highly photosynthetic *M. rubrum/major* species complex (Johnson et al. 2016, Peltomaa and Johnson 2017), but previous work has shown that these species (e.g., *Teleaulax* spp.) are either not retained (Moeller and Johnson 2018) or retained in very low abundances (Kim and Park 2019) by *M. chamaeleon* and *M. coatsi*, respectively. Divergent patterns of prey plastid retention may reflect niche partitioning by these two groups of *Mesodinium* ciliates, but prey

feeding preference assays are needed to determine whether these species are likely to compete for prey in field systems. By retaining functional plastids, *M. chamaeleon* also bolsters its growth and survival in the absence of prey, perhaps allowing it to tolerate short periods of starvation and survive in lower prey environments than the heterotrophic lineages *M. pulex* and *pupula*. Future work, including genetic studies, in this genus may help to resolve the ecological selection pressures that have produced a gradient of reliance on stolen chloroplasts.

We gratefully acknowledge feedback on early drafts of this manuscript from the members of the Moeller Lab at UC Santa Barbara and two anonymous reviewers. This work was funded by a Norma J. Lang Early Career Fellowship from the Phycological Society of America and a Hellman Faculty Fellowship (to HVM). Research was also sponsored by the U.S. Army Research Office and was accomplished under Cooperative Agreement Number W911NF-19-2-0026 for the Institute for Collaborative Biotechnologies. The views and conclusions contained in this document are those of the authors and should not be interpreted as representing the official policies, either expressed or implied, of the U.S. Government. The U.S. Government is authorized to reproduce and distribute reprints for Government purposes notwithstanding any copyright notation herein.

#### AUTHOR CONTRIBUTION

**H.V. Moeller:** Conceptualization (equal); data curation (lead); formal analysis (lead); funding acquisition (lead); investigation (lead); methodology (lead); project administration (lead); resources (lead); supervision (lead); validation (lead); visualization (lead); writing – original draft (lead); writing – review and editing (equal). **V. Hsu:** Investigation (supporting); methodology (supporting); writing – review and editing (supporting). **M. Lepori-Bui:** Investigation (supporting); methodology (supporting); supervision (equal); writing – review and editing (supporting). **L.Y. Mesrop:** Conceptualization (supporting); investigation (supporting); methodology (supporting); writing – review and editing (supporting). **C. Chinn:** Investigation (supporting); methodology (supporting); writing – review and editing (supporting). **M.D. Johnson:** Conceptualization (equal); formal analysis (supporting); methodology (supporting); writing – review and editing (equal).

#### DATA AVAILABILITY STATEMENT

Data and analysis files are available on GitHub (DOI: <http://doi.org/10.5281/zenodo.4361739>).

- Cunningham, B. R., Greenwold, M. J., Lachenmyer, E. M., Heidenreich, K. M., Davis, A. C., Dudycha, J. L. & Richardson, T. L. 2019. Light capture and pigment diversity in marine and freshwater cryptophytes. *J. Phycol.* 55:552–64.
- Deblois, C. P., Marchand, A. & Juneau, P. 2013. Comparison of photoacclimation in twelve freshwater photoautotrophs (Chlorophyte, Bacillariophyte, Cryptophyte and Cyanophyte) isolated from a natural community. *PLoS ONE* 8:e57139.
- Doust, A. B., Wilk, K. E., Curmi, P. M. G. & Scholes, G. D. 2006. The photophysics of cryptophyte light-harvesting. *J. Photochem. Photobiol. A: Chem.* 184:1–17.
- Flynn, K. J., Mitra, A., Anestis, K., Anschütz, A. A., Calbet, A., Ferreira, G. D., Gypens, N. et al. 2019. Mixotrophic protists and a new paradigm for marine ecology: where does plankton research go now? *J. Plankt. Res.* 41:375–91.
- García-Cuetos, L., Moestrup, Ø. & Hansen, P. J. 2012. Studies on the genus *Mesodinium* II. Ultrastructural and molecular investigations of five marine species help clarifying the taxonomy. *J. Euk. Microbiol.* 59:374–400.
- García-Portela, M., Riobó, P., Reguera, B., Garrido, J. L., Blanco, J. & Rodríguez, F. 2018. Comparative ecophysiology of *Dinophysis acuminata* and *D. acuta* (Dinophyceae, Dinophysiales): effect of light intensity and quality on growth, cellular toxin content, and photosynthesis. *J. Phycol.* 54:899–917.
- Gast, R. J., Dennett, M. R. & Caron, D. A. 2004. Characterization of protistan assemblages in the Ross Sea, Antarctica, by denaturing gradient gel electrophoresis. *Appl. Environ. Microbiol.* 70:2028–37.
- Gorbunov, M. Y., Kolber, Z. S. & Falkowski, P. G. 1999. Measuring photosynthetic parameters in individual algal cells by fast repetition rate fluorometry. *Photosynth. Res.* 62:141–53.
- Greenwold, M. J., Cunningham, B. R., Lachenmyer, E. M., Pullman, J. M., Richardson, T. L. & Dudycha, J. L. 2019. Diversification of light capture ability was accompanied by the evolution of phycobiliproteins in cryptophyte algae. *Proc. Royal Soc. B.* 286:20190655.
- Guillard, R. R. L. 1975. Culture of phytoplankton for feeding marine invertebrates. In Smith, W. L. & Chanley, M. H. [Eds.] *Culture of Marine Invertebrate Animals*. Plenum Press, New York, pp. 26–60.
- Gustafson, D. E., Stoecker, D. K., Johnson, M. D., Van Heukelem, W. F. & Sneider, K. 2000. Cryptophyte algae are robbed of their organelles by the marine ciliate *Mesodinium rubrum*. *Nature* 405:1049–52.
- Hansen, P. J., Moldrup, M., Tarangkoon, W., Garcia-Cuetos, L. & Moestrup, Ø. 2012. Direct evidence for symbiont sequestration in the marine red tide ciliate *Mesodinium rubrum*. *Aquat. Microb. Ecol.* 66:63–75.
- Hansen, P. J., Nielsen, L. T., Johnson, M., Berge, T. & Flynn, K. J. 2013. Acquired phototrophy in *Mesodinium* and *Dinophysis* – A review of cellular organization, prey selectivity, nutrient uptake and bioenergetics. *Harmful Algae* 28:126–39.
- Hansen, P. J., Ojamäe, K., Berge, T., Trampe, E. C. L., Nielsen, L. T., Lips, I. & Kühl, M. 2016. Photoregulation in a kleptochloroplastic dinoflagellate, *Dinophysis acuta*. *Front. Microbiol.* 7:37–11.
- Holling, C. S. 1959. Some characteristics of simple types of predation and parasitism. *Can. Entomol.* 91:385–98.
- Jakobsen, H. H., Everett, L. M. & Strom, S. L. 2006. Hydromechanical signaling between the ciliate *Mesodinium pulex* and motile protist prey. *Aquat. Microb. Ecol.* 44:197–206.
- Jassby, A. D. & Platt, T. 1976. Mathematical formulation of the relationship between photosynthesis and light for phytoplankton. *Limnol. Oceanogr.* 21:540–7.
- Jeong, H. J. & Latz, M. I. 1994. Growth and grazing rates of the heterotrophic dinoflagellates *Proto-peridinium* spp. on red tide dinoflagellates. *Mar. Ecol. Prog. Ser.* 106:173–85.
- Johnson, M. D. 2011a. Acquired phototrophy in ciliates: A review of cellular interactions and structural adaptations. *J. Euk. Microbiol.* 58:185–95.
- Johnson, M. D. 2011b. The acquisition of phototrophy: adaptive strategies of hosting endosymbionts and organelles. *Photosynth. Res.* 107:117–32.
- Johnson, M. D., Beaudoin, D. J., Laza-Martinez, A., Dyhrman, S. T., Fensin, E., Lin, S., Merculief, A., Nagai, S., Pompeu, M., Setälä, O. & Stoecker, D. K. 2016. The genetic diversity of *Mesodinium* and associated cryptophytes. *Front. Microbiol.* 7:108–16.
- Johnson, M., Oldach, D., Delwiche, C. & Stoecker, D. 2007. Retention of transcriptionally active cryptophyte nuclei by the ciliate *Myrionecta rubra*. *Nature* 445:426–8.

- Johnson, M. & Stoecker, D. 2005. Role of feeding in growth and photophysiology of *Myrionecta rubra*. *Aquat. Microb. Ecol.* 39:303–12.
- Johnson, M. D., Tengs, T., Oldach, D. & Stoecker, D. K. 2006. Sequestration, performance, and functional control of cryptophyte plastids in the ciliate *Myrionecta rubra* (Ciliophora). *J. Phycol.* 42:1235–46.
- Kim, M., Drumm, K., Daughjerg, N. & Hansen, P. J. 2017. Dynamics of sequestered cryptophyte nuclei in *Mesodinium rubrum* during starvation and refeeding. *Front. Microbiol.* 8:423.
- Kim, M., Kang, M. & Park, M. G. 2019. Growth and chloroplast replacement of the benthic mixotrophic ciliate *Mesodinium coatsi*. *J. Euk. Microbiol.* 66:1–12.
- Kim, M., Nam, S. W., Shin, W., Coats, D. W. & Park, M. G. 2012. *Dinophysis caudata* (Dinophyceae) sequesters and retains plastids from the mixotrophic ciliate prey *Mesodinium rubrum*. *J. Phycol.* 48:569–79.
- Kim, M., Nam, S. W., Shin, W., Coats, D. W. & Park, M. G. 2015. Fate of green plastids in *Dinophysis caudata* following ingestion of the benthic ciliate *Mesodinium coatsi*: Ultrastructure and psbA gene. *Harmful Algae* 43:66–73.
- Kim, M. & Park, M. G. 2019. Unveiling the hidden genetic diversity and chloroplast type of marine benthic ciliate *Mesodinium* species. *Sci. Rep.* 9:1–10.
- Lawrenz, E., Silsbe, G., Capuzzo, E., Ylöstalo, P., Forster, R. M., Simis, S. G. H., Prášil, O. et al. 2013. Predicting the electron requirement for carbon fixation in seas and oceans. *PLoS ONE* 8:e58137.
- Laws, E. A. 1991. Photosynthetic quotients, new production and net community production in the open ocean. *Deep Sea Res. Part A. Oceanog. Res. Papers.* 38:143–67.
- Lewitus, A. J. & Caron, D. A. 1990. Relative effects of nitrogen or phosphorus depletion and light intensity on the pigmentation, chemical composition, and volume of *Pyrenomonas salina* (Cryptophyceae). *Mar. Ecol. Prog. Ser.* 61:171–81.
- Long, S. P., Humphries, S. & Falkowski, P. G. 1994. Photoinhibition of photosynthesis in nature. *Ann. Rev. Plant Biol.* 45:633–62.
- MacIntyre, H. L., Kana, T. M., Anning, T. & Geider, R. J. 2002. Photoacclimation of photosynthesis irradiance response curves and photosynthetic pigments in microalgae and cyanobacteria. *J. Phycol.* 38:17–38.
- Moeller, H. V. & Johnson, M. D. 2018. Preferential plastid retention by the acquired phototroph *Mesodinium chamaeleon*. *J. Eukaryot. Microbiol.* 65:148–58.
- Moeller, H. V., Johnson, M. D. & Falkowski, P. G. 2011. Photoacclimation in the phototrophic marine ciliate *Mesodinium rubrum* (Ciliophora). *J. Phycol.* 47:324–32.
- Moeller, H. V., Peltomaa, E., Johnson, M. D. & Neubert, M. G. 2016. Acquired phototrophy stabilises coexistence and shapes intrinsic dynamics of an intraguild predator and its prey. *Ecol. Lett.* 19:393–402.
- Moestrup, Ø., Garcia-Cuetos, L., Hansen, P. J. & Fenchel, T. 2012. Studies on the genus *Mesodinium* I: Ultrastructure and description of *Mesodinium chamaeleon* n. sp., a benthic marine species with green or red chloroplasts. *J. Euk. Microbiol.* 59:20–39.
- Myung, G., Kim, H. S., Park, J. S., Park, M. G. & Yih, W. 2011. Population growth and plastid type of *Myrionecta rubra* depend on the kinds of available cryptomonad prey. *Harmful Algae* 10:536–41.
- Nam, S. W., Shin, W., Kang, M., Yih, W. & Park, M. G. 2014. Ultrastructure and molecular phylogeny of *Mesodinium coatsi* sp. nov., a benthic marine ciliate. *J. Euk. Microbiol.* 62:102–20.
- Park, J. S., Myung, G., Kim, H. S., Cho, B. C. & Yih, W. 2007. Growth responses of the marine photosynthetic ciliate *Myrionecta rubra* to different cryptomonad strains. *Aquat. Microb. Ecol.* 48:83–90.
- Peltomaa, E. & Johnson, M. D. 2017. *Mesodinium rubrum* exhibits genus-level but not species-level cryptophyte prey selection. *Aquat. Microb. Ecol.* 78:147–59.
- R Core Team. 2014. *R: A Language and Environment for Statistical Computing*. R Foundation for Statistical Computing, Vienna, Austria.
- Rogerson, A., Finlay, B. J. & Berninger, U. G. 1989. Sequestered chloroplasts in the freshwater ciliate *Strombidium viride* (Ciliophora: Oligotrichida). *Trans. Am. Microscopical Soc.* 108:117.
- Schoener, D. M. & McManus, G. B. 2012. Plastid retention, use, and replacement in a kleptoplastidic ciliate. *Aquat. Microb. Ecol.* 67:177–87.
- Smith, M. & Hansen, P. 2007. Interaction between *Mesodinium rubrum* and its prey: importance of prey concentration, irradiance and pH. *Mar. Ecol. Prog. Ser.* 338:61–70.
- Stoecker, D. K. 1998. Conceptual models of mixotrophy in planktonic protists and some ecological and evolutionary implications. *Eur. J. Protistol.* 34:281–90.
- Stoecker, D. K., Johnson, M. D., deVargas, C. & Not, F. 2009. Acquired phototrophy in aquatic protists. *Aquat. Microb. Ecol.* 57:279–310.
- Stoecker, D. K. & Silver, M. W. 1990. Replacement and aging of chloroplasts in *Strombidium capitatum* (Ciliophora: Oligotrichida). *Mar. Biol.* 107:491–502.
- Tarangkoon, W. & Hansen, P. J. 2011. Prey selection, ingestion and growth responses of the common marine ciliate *Mesodinium pulex* in the light and in the dark. *Aquat. Microb. Ecol.* 62:25–38.
- Vieira, S., Calado, R., Coelho, H. & Serôdio, J. 2009. Effects of light exposure on the retention of kleptoplastic photosynthetic activity in the sacoglossan mollusc *Elysia viridis*. *Mar. Biol.* 156:1007–20.

### Supporting Information

Additional Supporting Information may be found in the online version of this article at the publisher's web site:

**Figure S1.** Population dynamics and chlorophyll content of *Mesodinium chamaeleon* acclimated to *Chroomonas mesostigmatica*. Data for fed (black lines and symbols) and starved (gray lines and symbols) treatments are shown. Top row: *M. chamaeleon* cell densities over time. Second row: Cryptophyte cell densities over time. Third row: Plastid content over time. Fourth row: *M. chamaeleon* per-cell chlorophyll-*a* content over time. Fifth row: *M. chamaeleon* per-carbon chlorophyll-*a* content over time. Bottom row: Total chlorophyll-*a* content (per mL) in *M. chamaeleon* cells over time. Points show means, with error bars representing +/- one standard error.

**Figure S2.** Population dynamics and chlorophyll content of *Mesodinium chamaeleon* acclimated to *Hemiselmis pacifica*. Data for fed (black lines and symbols) and starved (gray lines and symbols) treatments are shown. Top row: *M. chamaeleon* cell densities over time. Second row: Cryptophyte cell densities over time. Third row: Plastid content over time. Fourth row: *M. chamaeleon* per-cell chlorophyll-*a* content over time. Fifth row: *M. chamaeleon* per-carbon chlorophyll-*a* content over time. Bottom row: Total chlorophyll-*a* content (per mL) in *M. chamaeleon* cells over time. Points show means, with error bars representing +/- one standard error.

**Figure S3.** Population dynamics and chlorophyll content of *Mesodinium chamaeleon* acclimated

to *Rhodomonas salina*. Data for fed (black lines and symbols) and starved (gray lines and symbols) treatments are shown. Top row: *M. chamaeleon* cell densities over time. Second row: Cryptophyte cell densities over time. Third row: Plastid content over time. Fourth row: *M. chamaeleon* per-cell chlorophyll-*a* content over time. Fifth row: *M. chamaeleon* per-carbon chlorophyll-*a* content over time. Bottom row: Total chlorophyll-*a* content (per mL) in *M. chamaeleon* cells over time. Points show means, with error bars representing  $\pm$  one standard error.

**Figure S4.** Population dynamics and chlorophyll content of *Mesodinium chamaeleon* acclimated to *Storeatula major*. Data for fed (black lines and symbols) and starved (gray lines and symbols) treatments are shown. Top row: *M. chamaeleon* cell densities over time. Second row: Cryptophyte cell densities over time. Third row: Plastid content over time. Fourth row: *M. chamaeleon* per-cell chlorophyll-*a* content over time. Fifth row: *M. chamaeleon* per-carbon chlorophyll-*a* content over time. Bottom row: Total chlorophyll-*a* content (per mL) in *M. chamaeleon* cells over time. Points show means, with error bars representing  $\pm$  one standard error.

**Figure S5.** Photosynthetic capacity of *Mesodinium chamaeleon* acclimated to *Chroomonas mesostigmatica*. Data for fed (black lines and symbols) and starved (gray lines and symbols) treatments are shown. Prey data (colored lines and symbols) are overlaid for reference. Top row: *M. chamaeleon* photosynthetic efficiency (Fv/Fm). Second row:  $\alpha^B$ , the slope of the photosynthesis-irradiance curve normalized to chlorophyll-*a*. Third row:  $P_{\max,chl}$ , the maximum photosynthetic rate normalized to chlorophyll-*a*. Final three rows: Carbon fixation rates at growth irradiance normalized to chlorophyll-*a* (fourth row), carbon (fifth row), and cell (bottom row). Points show means, with error bars representing  $\pm$  one standard error.

**Figure S6.** Photosynthetic capacity of *Mesodinium chamaeleon* acclimated to *Hemiselmis pacifica*. Data for fed (black lines and symbols) and starved (gray lines and symbols) treatments are shown. Prey data (colored lines and symbols) are overlaid for reference. Top row: *M. chamaeleon* photosynthetic efficiency (Fv/Fm). Second row:  $\alpha^B$ , the slope of the photosynthesis-irradiance curve normalized to chlorophyll-*a*. Third row:  $P_{\max,chl}$ , the maximum photosynthetic rate normalized to chlorophyll-*a*. Final three rows: Carbon fixation rates at growth irradiance normalized to chlorophyll-*a* (fourth row), carbon (fifth row), and cell (bottom row). Points show means, with error bars representing  $\pm$  one standard error.

**Figure S7.** Photosynthetic capacity of *Mesodinium chamaeleon* acclimated to *Rhodomonas salina*. Data for fed (black lines and symbols) and starved (gray lines and symbols) treatments are shown. Prey data (colored lines and symbols) are overlaid for reference. Top row: *M. chamaeleon* photosynthetic efficiency (Fv/Fm). Second row:  $\alpha^B$ , the slope of the photosynthesis-irradiance curve normalized to chlorophyll-*a*. Third row:  $P_{\max,chl}$ , the maximum photosynthetic rate normalized to chlorophyll-*a*. Final three rows: Carbon fixation rates at growth irradiance normalized to chlorophyll-*a* (fourth row), carbon (fifth row), and cell (bottom row). Points show means, with error bars representing  $\pm$  one standard error.

**Figure S8.** Photosynthetic capacity of *Mesodinium chamaeleon* acclimated to *Storeatula major*. Data for fed (black lines and symbols) and starved (gray lines and symbols) treatments are shown. Prey data (colored lines and symbols) are overlaid for reference. Top row: *M. chamaeleon* photosynthetic efficiency (Fv/Fm). Second row:  $\alpha^B$ , the slope of the photosynthesis-irradiance curve normalized to chlorophyll-*a*. Third row:  $P_{\max,chl}$ , the maximum photosynthetic rate normalized to chlorophyll-*a*. Final three rows: Carbon fixation rates at growth irradiance normalized to chlorophyll-*a* (fourth row), carbon (fifth row), and cell (bottom row). Points show means, with error bars representing  $\pm$  one standard error.

**Figure S9.** Photosynthesis-irradiance curves for starved *Mesodinium chamaeleon* cells. Photosynthetic activity is measured as electron transport rate (electrons transported per second by each molecule of chlorophyll-*a*). Treatments are grouped by plastid type (columns) and light level (rows: top = 10, middle = 50, bottom = 100  $\mu\text{mol quanta} \cdot \text{m}^{-2} \cdot \text{s}^{-1}$ ). Lines (which represent the best fit hyperbolic tangent curves) are color coded by timepoint: black represents Day 0, and shades lighten as timepoints progress.

**Figure S10.** Photosynthesis-irradiance curves for starved *Mesodinium chamaeleon* cells. Photosynthetic activity is measured as carbon fixation per carbon (mg of carbon fixed per hour per each *M. chamaeleon* g C). Treatments are grouped by plastid type (columns) and light level (rows: top = 10, middle = 50, bottom = 100  $\mu\text{mol quanta} \cdot \text{m}^{-2} \cdot \text{s}^{-1}$ ). Lines (which represent the best fit hyperbolic tangent curves) are color coded by timepoint: black represents Day 0, and shades lighten as timepoints progress.

**Figure S11.** Relative performance of *Mesodinium chamaeleon* compared to its prey. Symbols are colored by prey type, and represent means (with error bars indicating  $\pm$  one standard error) across light levels (*x*-axis). A: *M. chamaeleon*

photosynthetic efficiencies increased relative to prey with increasing light for *Rhodomonas salina* and *Chroomonas mesostigmatica*. B: *M. chamaeleon* light sensitivity ( $\alpha^B$ ) was lower than cryptophytes except for *Hemiselmis pacifica* at intermediate and high light levels. C: For all four prey types, maximum photosynthetic rates declined relative to prey rates with increasing light. D: Except for *C. mesostigmatica*, this was also true for in situ photosynthetic rates.

**Figure S12.** Cellular carbon content of *Mesodinium chamaeleon* (A, grouped by prey plastid type) and cryptophytes (B) measured at  $10 \mu\text{mol quanta} \cdot \text{m}^{-2} \cdot \text{s}^{-1}$ . Bar heights represent means, and error bars represent  $\pm$  one standard error. Letters indicate significant differences at the  $P < 0.05$  level (Tukey's HSD).